Polym. Korea, Vol. 46, No. 6, pp. 728-743 (2022)
https://doi.org/10.7317/pk.2022.46.6.728

ISSN 0379-153X(Print)
ISSN 2234-8077(Online)

표면 개질된 Halloysite 나노튜브(mHNTs)가 EPDM/NBR 나노복합체의 기계적 물성 및 팽윤 거동에 미치는 영향

R. Sundar†, S. Krishna Mohan, and S. Vishvanathperumal*

Department of Mechanical Engineering, E.G.S. Pillay Engineering College

*Department of Mechanical Engineering, S.A. Engineering College

(2022년 5월 19일 접수, 2022년 8월 5일 수정, 2022년 8월 30일 채택)

Effect of Surface Modified Halloysite Nanotubes (mHNTs) on the Mechanical Properties and Swelling Resistance of EPDM/NBR Nanocomposites

R. Sundar†, S. Krishna Mohan, and S. Vishvanathperumal*

Department of Mechanical Engineering, E.G.S. Pillay Engineering College, Nagappattinam, Tamilnadu 611002, India

**Department of Mechanical Engineering, S.A. Engineering College, Chennai, Tamilnadu 600077, India*

(Received May 19, 2022; Revised August 5, 2022; Accepted August 30, 2022)

Abstract: Ethylene-propylene-diene monomer/acrylonitrile-butadiene rubber (EPDM/NBR)-modified halloysite nanotubes (mHNTs) nanocomposites were prepared by two-roll mixing mill and vulcanization process. The mole percent uptake of some aromatic (toluene, xylene, benzene and mesitylene), aliphatic (*n*-hexane, *n*-heptane, *n*-octane and *n*-pentane) and chlorinated (chloroform, carbon tetrachloride and dichloromethane) solvents through mHNT filled EPDM/NBR nanocomposites has been investigated. The aim of the present work is to investigate the role of the cure characteristics, mechanical properties, abrasion resistance and swelling resistance in analysing the compatibility between rubber matrix and nanotubes and the reinforcing effect of mHNT as nanofiller in the EPDM/NBR matrix. The mole percent uptake of organic solvents *via* membranes has been explored in detail as a function of mHNT content, type of solvent, and temperature between 23 and 60 °Celsius. The findings revealed that mHNT could reduce scorch and optimum cure time in EPDM/NBR vulcanizates, as well as play a significant role in strengthening EPDM/NBR vulcanizates. Mechanical properties and swelling resistance were investigated and were found to increase with the increase of mHNT loading. The cross-link density values indicated the improved strengthening at 8 phr mHNT filler loading. In the rubber matrix, mHNT particles form a local filler–filler network at high concentrations. As a result, the composites' mechanical properties were greatly improved.

Keywords: ethylene-propylene-diene monomer/acrylonitrile-butadiene rubber, modified halloysite nanotube, mechanical properties, swelling properties.

Introduction

Rubber's reinforcing particulate fillers have been investigated extensively in the past. Carbon black (CB) and silica (SiO_2) are the most commonly used fillers in rubber compounds, especially tyres, due to their high reinforcing properties based on structure and physical bonding with rubber for the former and good friction properties with low rolling resistance for the latter.[1-6] Several innovative filler systems have been researched to overcome the limits and drawbacks of present filler systems since the significant rise in nanoscience and technology.[7-9] Smart materials with great performance and versatility are among the new generation of materials that have attracted attention. The production of elastomer nanocomposites is significant in the production of such materials and represents one of the most significant areas of current nanotechnology and composite science. Their beneficial applications have sparked in-depth research in both theoretical and applied fields. Nanofillers like CB, silica, layered silicates, titanium dioxide (TiO_2), carbon nanotubes (CNTs), graphene and polyhedral oligomeric silsesquioxane (POSS) have been added to different elastomer matrices to provide effective reinforce-

†To whom correspondence should be addressed.
sundar@egspec.org, ORCID 0000-0001-5721-549X

ment and functional properties for the creation of elastomer nanocomposites. Due to their multifunctional characteristics, nanotube-based filler systems stand out among other nanocomposite systems. All elastomer matrices can benefit from improved mechanical and tribological, thermal, and gas barrier qualities. This review tries to give a complete grasp of their structures and properties in the context in which they are discussed.

Because of their outstanding mechanical properties, increased thermal properties, and other functionalities, polymer/inorganic materials have gotten a lot of attention.[10-13] According to their geometrical dimension, inorganic nanofillers are classified as one-dimensional fillers, two-dimensional fillers, and three-dimensional particles. Furthermore, the shape and structure of the filler have a considerable impact on the composites' final performance. Nanofiller-based polymer composites have emerged as one of the most appealing areas in material research. Halloysite nanotubes (HNTs) have gotten a lot of attention in the research community because of some of their interesting intrinsic features.[14] HNTs with primarily hollow tubular nanostructures and high aspect ratios[15,16] are frequently employed in composites as an environmentally acceptable natural nanofiller. Natural HNTs are readily available and substantially less expensive than alternative nanosized inorganic fillers.[17,18]

HNT is a clay mineral made up of kaolin that is abundant in nature. It's an aluminium silicate with the chemical formula $[Al_2Si_2O_5(OH)_4]$. It features a hollow tubular structure with an Al-OH inner surface and a Si-O-Si exterior surface.[19,20] HNT is an electrophilic substance due to the presence of Al- in its structure.[21] Halloysite materials have been known for a long time, but widespread study using HNTs has only lately begun. HNTs are appropriate for a wide range of applications due to their excellent mechanical qualities, high aspect ratio, low cost, good compatibility with various polymer materials, low volume to weight ratio and high surface area.[22-27] Nanocomposites and enzyme immobilisation,[28] gas separation,[29] water purification,[30] antimicrobial coatings,[31] and halogen-free flame retardants[32,33] are just a few of the uses for HNT. HNT was employed as a reinforcing nanofiller material for green composites by Rooj *et al.* (2010), and as a nanofiller by Du *et al.* (2008) to promote interfacial bonding in nanocomposites by Du *et al.* (2008).[34,35]

As a result, both pristine and modified HNTs can be used as a potential inorganic filler in polymer matrix to provide excellent mechanical and thermal properties.[36,37] Many researchers have explored the nanocomposites generated by HNT and many polymers since then, including polypropylene,[38] chitosan,[39,40] epoxy resin,[41,42] nylon,[43] polystyrene,[44] polyethylene,[45] polyvinyl alcohol (PVOH),[46] polyvinyl chloride (PVC),[47] rubbers,[48] and so on. HNT has considerable strengthening and modifying effects on polymers, according to the findings.[49] Rubbers researched include natural rubber (NR),[50,51] styrene-butadiene rubber (SBR),[52] carboxylated styrene butadiene rubber,[53] acrylonitrile-butadiene rubber (NBR),[54] ethylene-propylene-diene monomer (EPDM),[55-57] and fluororubber,[58] among others. The addition of an interfacial modifier to disseminate HNT in the rubber matrix and improve the interfacial interaction between HNT and rubber is a typical feature of these rubber/HNT composites. Interfacial modifiers that have been described include a resorcinol and hexamethylenetetramine (RH) complex,[59] epoxidized NR (ENR)m[60] methacrylic acid (MAA),[61] sorbic acid ($CH_3(CH)_4CO_2H$),[62] and others. RH and ENR, interfacial modifiers, have been shown to increase nanodispersion and orientation of HNT in rubber matrix in previous studies,[59,60] They can also create hydrogen and covalent interactions, which increase the interfacial interaction between HNT and the rubber matrix.

The rubber matrix and the filler are connected to one other through physical interactions in rubber-based nanocomposites without interfacial modifiers, and interfacial covalent bonding is rarely used. Nanocomposites with significantly better characteristics can be made if the filler is disseminated at the nanoscale level in the rubber matrix and the interface between the two phases creates chemical bonding. Because the polar groups on the surface of HNT particles are smaller than those on silica, particle agglomeration is less severe. As a result, HNT disperses in rubber more easily than silica without the use of an interfacial modifier. Tubular nanoparticles can also position themselves in the rubber matrix, improving the mechanical properties of nanocomposites.

The major goal of this research is to investigate into the benefits of using an experimental technique to analyse the compatibility and reinforcing effect of HNTs as a filler in an EPDM/NBR (ethylene-propylene-diene monomer/acrylonitrile butadiene rubber) matrix. To our knowledge, no research on the cure, mechanical behaviour, and swelling resistance of modified-halloysite nanotubes (mHNTs) in an EPDM/NBR rubber matrix has been published. EPDM is a non-polar, high-density, saturated rubber with a number of beneficial qualities such as heat stability, light, ozone, ageing, steam, weather and water resistance. NBR, on the other hand, is a butadiene and

acrylonitrile random copolymer. It is one of the most essential industrial raw materials due to its strong polarity and polar CN groups.[63] However, as compared to EPDM, its mechanical qualities are inferior. The physico-mechanical properties of (EPDM/NBR) rubber blends crosslinked with Sulfur/accelerator and compatilized by EPDM-*g*-MA and modified-HNTs in various ratios were studied. The surface modification of HNTs or the interfacial modification of composites are the focus of these studies. RH was used as an interfacial modification of HNTs in the preparation of modified HNTs (m-HNTs) and EPDM/NBR/mHNT nanocomposites in this study. The effects of penetrant size, filler (modified-HNTs) loading, penetrant type, and temperature on the mole percent uptake of solvents through EPDM/NBR nanocomposite membranes are investigated in this study. The dispersion of HNTs has been intensively examined by field emission scanning electron microscopy (FESEM) in order to connect the morphology with the tensile strength. Tensile tests on EPDM/NBR composites modified with different HNTs filler ratios revealed that the EPDM/NBR (75/25 phr/phr) blend was the best, with the best mechanical properties; however, pure EPDMs, both filled and unfilled, had even better properties.[64-66] This blend composition composite was chosen to explore the qualities and structures of the blends.

Experimental

Materials. Ethylene-propylene-diene monomer (EPDM) rubber, family: terpolymer, Grade: KEP 270, ethylidene norbornene (ENB): 4.5%, ethylene content: 57%, Mooney viscosity (MV) ML(1+4) at 125 °C: 71 M, density: 0.86 g/cm^3,[67] was obtained from Supple Rubber Chemicals Private Limited, Faridabad, Haryana, India.

The acrylonitrile butadiene rubber (NBR), family: copolymer, Grade: KUMHO KNB 35L, acrylonitrile content (ACN): 34% butadiene content: 66%, density: 0.98 g/cc, MV ML(1+4) at 100 °C: 41 M was obtained from Apar Industries Ltd., Mumbai, India.

Halloysite nanotube (HNT) is one of the utmost multipurpose nanofillers used in compounding elastomers. It provides a range of mechanical qualities while also acting as effective and moderately inexpensive nanofillers (in comparison to carbon nanotubes (CNTs)) for increasing the general properties of rubber mixes. HNTs with formula $Al_2Si_2O_5(OH)_4 \cdot 2H_2O$, density: 2.53 g/cm^3, molecular weight: 294.19 g/mol was obtained from Sigma-Aldrich, Puducherry, India.

All other ingredients,[68] zinc oxide (ZnO) added to the elastomer compounds to activate sulphur (crosslinking agent) vulcanization and thus reduce the vulcanization time, dibenzthiazyl disulphide (MBTS), tetramethylthiuram disulfide (TMTD) are used as a vulcanization accelerator to increase the mechanical and thermal characteristics and ageing resistance of rubber vulcanizates by increasing the rate of cure, stearic acid used as accelerator and activator, softener and dispersing agent in rubber compounds, were obtained from Vignesh Chemicals, Chennai, India and used as obtained.

Ethylene-propylene-diene monomer-grafted-maleic anhydride (EPDM-*g*-MA), trademark name: Bondyram® 7001, used as a compatibilizer, melt flow rate: 7 g/10 min, maleic anhydride (MH) content: 0.7%, mass density: 0.87 g/cm^3 was purchased from Songhan Plastic Technology Co. Ltd., Shanghai City, China.

The complex of resorcinol and hexamethylenetetramine (RH) is from Shanghai Meclin Biochemical Technology Co., Ltd., China.

Solvents[69] such as hexane, heptane, octane, pentane, toluene, xylene, benzene, mesitylene, chloroform, carbon tetrachloride and dichloromethane used in this investigation were of Merck grade conquered from Sigma-Aldrich, Puducherry, India.

Surface Modification of HNTs. Because the surfaces of HNTs are hydrophilic and most polymer surfaces are hydrophobic, there is poor compatibility between the two materials. It is required to change the surfaces of HNTs and improve their compatibility with polymers. The conditions for surface modification are provided by the activity of the hydroxyl groups and Si-O bonds on the surfaces of HNTs. HNT surfaces may be altered by interactions between modifiers and hydroxyl groups or through the adsorption and charge-transfer properties of modifiers on Si-O bonds.

The pristine HNTs were surface-treated by RH complex. The mass ratio of RH/HNTs was typically 6/100. This was accomplished by dissolving 0.6 gm of RH complex in 100 cc of distilled water at 60 °C and stirring until the RH complex was completely dissolved. The HNTs were then distributed in a stirred solution for 4 hours at 60 °C. The mixture was filtered after cooling to room temperature. These modified HNTs were dried in a vacuum oven for the entire night at 80 °C.[70.]

Characterization of the Modified HNTs Fillers. Through an immersion test, changes in surface polarity were investigated. A little amount of filler was added to the surface of a solvent, in this case water, to conduct the test. Due to their hydrophilic surfaces, the original HNTs sink right away,

Table 1. Formulation of the EPDM/NBR Blends Reinforced with HNT and mHNT

Sample code	Ingredients (phr)								
	EPDM	NBR	HNTs	mHNTs	ZnO	Stearic acid	MBTS	TMTD	Sulphur
H_0	75	25	0	-	4	1.5	1.2	1	2.5
H_2	75	25	2	-	4	1.5	1.2	1	2.5
H_4	75	25	4	-	4	1.5	1.2	1	2.5
H_6	75	25	6	-	4	1.5	1.2	1	2.5
H_8	75	25	8	-	4	1.5	1.2	1	2.5
H_{10}	75	25	10	-	4	1.5	1.2	1	2.5
mH_0	75	25	-	0	4	1.5	1.2	1	2.5
mH_2	75	25	-	2	4	1.5	1.2	1	2.5
mH_4	75	25	-	4	4	1.5	1.2	1	2.5
mH_6	75	25	-	6	4	1.5	1.2	1	2.5
mH_8	75	25	-	8	4	1.5	1.2	1	2.5
mH_{10}	75	25	-	10	4	1.5	1.2	1	2.5

whereas the modified fillers should float for a longer period of time. A water penetration test produced more precise data. This test involved filling a glass column with 0.02 g of filler and covering the opening with two layers of a hydrophobic filter with a pore size of 0.2 μm. The column was submerged in water, and the weight shift brought on by water absorption was tracked over time.

Preparation of Nanocomposites. In a laboratory scale open mill mixing mill (two-roll mixer) with a friction ratio of 1.25:1, EPDM, NBR, and mHNTs were mixed. The formulations of different mixes are given in Table 1. An oscillating die rheometer (ODR) was used to determine the cure qualities of the compounded samples at a temperature of 160 °C. After that, the samples were moulded in an electrically heated-semi-automated-hydraulic press at a constant pressure of 60 MPa and a constant temperature of 160 °C. Samples were synthesized with varied HNT loadings and identified as H_0, H_2, H_4, H_6, H_8, H_{10}, and similarly, samples were synthesized with varying mHNT loadings and identified as mH_0, mH_2, mH_4, mH_6, mH_8, mH_{10}. The phr (parts per hundred rubber) of HNT utilised per 500 g of rubber is indicated by the subscript.

Experimental Techniques. On an oscillating disc rheometer (ODR), the cure characteristics were assessed. Using TechPro Rheotech ODR, the cure characteristics (cure rate index, optimum cure time, scorch time, minimum torque, maximum torque and delta torque) of the various nanocomposites were investigated and are listed in Table 1 (as per ASTM D-2084). To generate roughly 2 mm thick sheets, compounds were vulcanised at 160 °C for the optimum cure period in a hydraulic compression press at 60 MPa.

The tensile properties (tensile strength (TS), elongation at break (EB), and 100% modulus (M100)) and tear strength were determined using a universal tensile testing machine (UTM) (Dak System Inc (model: T-72102), series 7200). Dumbbell specimens of 6 mm width and 33 mm gauge length were punched out of a compression moulded sheet using a dumb-bell shaped die along the mill direction to evaluate the tensile properties of the nanocomposites. According to ASTM D-412 and ASTM D-624 standards, tensile characteristics and tear strength were measured on a UTM at a cross head speed of 500 mm/min and at room temperature (23 °C). The average value obtained for five specimens is reported for each nanocomposite.

Hardness of the rubber samples was measured by a Sore A durometer (hardness tester) following ASTM D-2240 standard. As per ASTM D-2632 and ASTM D-5963, the rebound resilience and abrasion resistance of the rubber composite were determined, respectively.

The morphology of the nanocomposites was analysed by FESEM (field emission-scanning electron microscopy). The FESEM was run at a 200 kV accelerating voltage.

A round-edged steel die was used to cut rectangular samples with curved edges from the vulcanised sheets. A screw gauge was used to measure the thickness of the sample at numerous places. These samples were weighed before being immersed in 30 mL of solvent in diffusion bottles. At regular intervals, sam-

ples were removed from the bottles, the clinging solvent was gently blotted off the surface, and the samples were instantly weighed on a very sensitive electronic scale. Weighed samples were poured into the test vial right away. Weighing was continued until the swelling reached equilibrium. Weighing must be done within 30 seconds to avoid errors caused by evaporation of the solvent. Mole percent uptake properties were investigated using different solvents at four distinct temperatures: 23, 40, 50, and 60 °C.

Compression set tests were done utilising the dimensions of the specimen (diameter: 29 ± 0.5 mm and thickness: 12 ± 0.5 mm) and a compression set test according to ASTM D-395. Specimens were put between the plates of the compression apparatus for the compression set test, with a spacer on either side to allow for bulging rubber when compressed. The bolts were tightened until the plates were evenly drawn together and in contact with the spacer. For the test, a quarter (25% or 1/4th) of the specimen's original height was used. The constructed compression mechanism was then placed in an air-circulated oven for 22 hours at 23 and 72 °C. After a predetermined amount of time in the oven, specimens were taken from the device and allowed to cool for 30 minutes at room temperature before being measured for compression set.

$$\text{Compression set, } C = \frac{C_0 - C_1}{C_0 - C_S} \times 100 \quad (1)$$

where, C_0: original height of the rubber compound, C_1: compressed height of the rubber compound, C_S: height of the slip gauge or spacer.

Results and Discussion

Filler Characterization. The water immersion test was done to determine whether the hydrophobicity has changed. As anticipated, the untreated HNT powder instantly sank in water; but, following treatment, some of the substance floated on the water for a while. This demonstrates the decrease in polarity of the HNTs following RH modification, but it also shows an uneven coating, which may be brought on by the inclusion of filler aggregates in the RH modification process. Figure 1 displays the results of the water absorption. Both unmodified and RH-modified HNTs gradually absorbed water, and after a while, an equilibrium level was reached. However, pure HNTs absorbed more water than RH modified HNTs, suggesting that RH modified HNTs are more hydrophobic. This exploratory study showed that DMS modified HNTs are less polar and more hydrophobic than the unmodified filler, suggesting that they might work better with a non-polar rubber matrix.

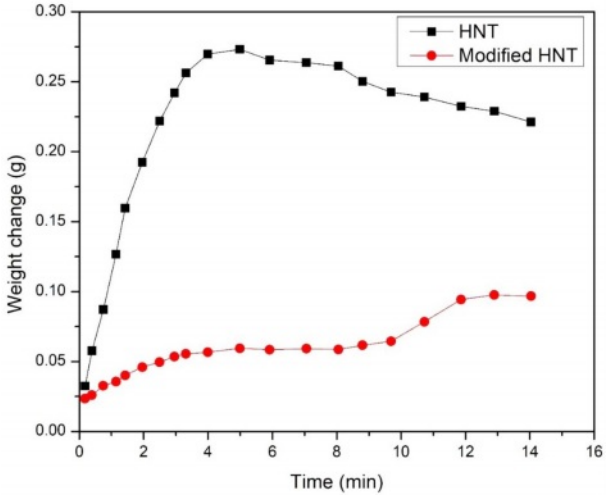

Figure 1. Water absorption of the modified HNTs.

Cure Characteristics of EPDM/NBR Nanocomposites. Table 2 summarises the results of the cure characteristics according to various HNTs ratios. When HNT or mHNT were introduced to rubber nanocomposites, it worked as an accelerator in the curing process, as evidenced by the reduction in optimum cure time and scorch time. In mHNT and sulphur-containing compounds, RH (complex of resorcinol and hexamethylenetetramine) was found to participate in the creation of zinc complex, which expedited the rubber curing process. However, because the sulphur concentration in the rubber formula was controlled, the optimal cure time and scorch time did not vary considerably as HNT content increased. Because the torque difference only slightly increased when HNT was added, it had little effect on crosslink density of the rubber composite. However, the mechanism behind it has yet to be discovered. The resorcinol-hexamethylenetetramine (RH) combination is commonly utilised to improve inorganic filler adherence in polymer matrices. RH has been shown to promote filler dispersion in addition to enhancing adhesion.[59] Jia *et al.*[59] looked at the relationship between the structure and characteristics of mHNT/SBR composites made using the direct blending method. They discovered that RH improved silicate dispersion and increased interfacial adhesion. These modified fillers improved the properties of the rubber matrix, according to rheometric and mechanical data, especially in the context of HNT in SBR. As a result, RH was introduced during masterbatch preparation in this section to increase rubber-HNT adhesion. In the rubber sector, RH is commonly

Table 2. Cure Characteristics of the EPDM/NBR Blends Reinforced with HNT and mHNT Compounds

Sample code	Min. torque (dN m)	Max. torque (dN m)	Torque difference (dN m)	Scorch time (min)	Optimum cure time (min)	Cure rate index (min^{-1})
H_0	0.17	0.49	0.32	0.61	3.34	36.63
H_2	0.19	0.52	0.33	0.58	3.15	38.91
H_4	0.21	0.54	0.33	0.55	3.04	40.16
H_6	0.23	0.57	0.34	0.51	2.91	41.67
H_8	0.24	0.6	0.36	0.49	2.85	42.37
H_{10}	0.24	0.62	0.38	0.48	2.82	42.74
mH_0	0.17	0.49	0.32	0.61	3.34	36.63
mH_2	0.21	0.56	0.35	0.52	2.88	42.37
mH_4	0.25	0.62	0.37	0.48	2.79	43.29
mH_6	0.28	0.68	0.4	0.44	2.54	47.62
mH_8	0.3	0.71	0.41	0.43	2.45	49.5
mH_{10}	0.32	0.73	0.41	0.41	2.41	50

employed as an adhesive. RH was first introduced to nitrile-butadiene rubber-organomontmorillonite (NBR-HMMT) nanocomposites as an interfacial modification by Liu and Jia *et al.*[71] The mechanical properties of the NBR-RH-HMMT nanocomposites were much superior than those of NBR-HMMT composites, according to the findings. Through interactions with NBR and modified clay, RH could improve the interface combination between the rubber and the organoclay. The curing characteristics of EPDM/NBR-mHNT compounds with varying mHNT concentrations are shown in Table 2. The optimum cure time, scorch time, cure rate index, minimum torque (ML), maximum torque (MH), and torque difference (M= MH-ML) were found to be somewhat altered at all contents of mHNT. As a result, the alteration of HNT by RH had an effect on the cure characteristics of EPDM/NBR nanocomposites. This could be because the amount of RH used to strengthen EPDM/NBR rubber was significantly higher than the amount of HNT used to reinforce EPDM/NBR rubber. As a result, the RH-induced response was considerably stronger than that of unaltered nanocomposites.

Mechanical Properties of EPDM/NBR Nanocomposites. Tensile Strength: Figure 2 shows the tensile strength results of EPDM/NBR-HNTs samples with various HNTs content. When HNT was introduced to EPDM/NBR, the tensile strength improved marginally. The addition of mHNT to EPDM/NBR nanocomposites resulted in an increase in tensile strength of the EPDM/NBR. Tensile strength of EPDM/NBR-mHNT nanocomposites improved as mHNT content increased. The enhanced contact between mHNT and EPDM/NBR rubber matrix, as well as the high aspect ratio of mHNT, which provided more surface area for the interaction between mHNT and EPDM/NBR rubber matrix, were deemed to be key contributors in the improvement in tensile strength. This allows the imparted stress to be effectively transferred to the modifier (RH) on the HNT's nanotubes. The inclusion of mHNT enhanced the tensile strength of EPDM/NBR rubber. The figures clearly demonstrated that as untreated HNT and RH treated HNT (mHNT) loading increased, tensile strength increased as well. When compared to the unfilled EPDM/NBR blend and EPDM/NBR filled with untreated HNT, the nanocomposites filled with mHNT had greater tensile strengths. When up to 6 phr of mHNT is applied, the tensile strength increases dramatically to 185 percent. However, nanocomposites with the largest amount of untreated HNT showed a decrease in tensile strength. As painstakingly seen in FESEM, this was attributed to platelet agglomeration and aggregation, which led in premature failure. Another reason could be that fine nanotubes aligned themselves in the direction of the stress, resulting in an increase in tensile strength. Furthermore, as compared to an unfilled EPDM/NBR mix, EPDM/NBR filled with untreated HNT demonstrated a similar optimal HNT loading of 6 phr and a tensile strength enhancement of up to 83 percent. The mechanical performance of EPDM/NBR blends was improved after surface treatment of HNT with RH. The combination of resorcinol and hexamethylenetetramine adsorbed on the HNT surface caused retention effects among

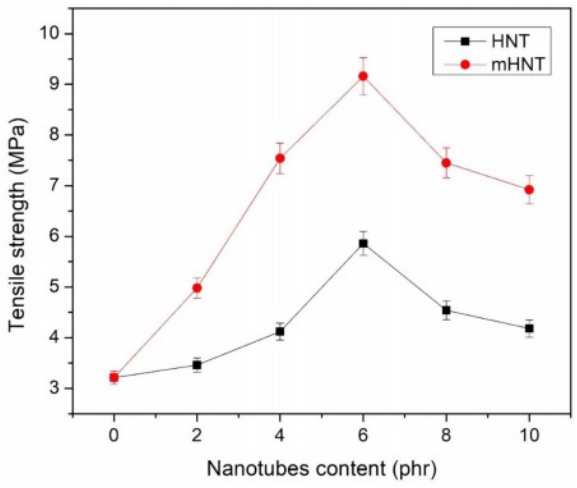

Figure 2. Tensile strength of EPDM/NBR blends with HNT and mHNT composites.

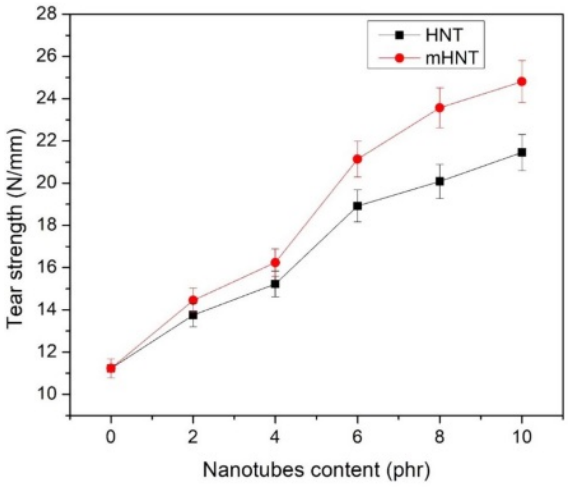

Figure 4. Tear strength of EPDM/NBR blends with HNT and mHNT composites.

HNT and improved separation. Aluminum hydroxide silicate-containing groups in the nanotubes introduced polar interactions between HNT and RH substances and non-polar (EPDM)/polar (NBR) polymer matrices. At greater loadings of HNT, however, limited functional groups on HNT surfaces induced selective distribution of HNT into high-polarity EPDM phases rather than the NBR phase. At 8 phr of untreated HNT loading in EPDM/NBR rubber matrix, this resulted in an uneven tensile loading that eventually resulted in a loss in strength.

Elongation at Break: The elongation at break curves of the vulcanizates EPDM/NBR, EPDM/NBR-HNT, and EPDM/NBR-mHNT are shown in Figure 3. The data in Figure 3 show that as the weight fraction of HNT in the systems was increased, the extensibility of various rubber compounds monotonically decreased with increasing elongation at break. The data in Figure 3 for modified HNTs demonstrate that, up to 6 phr, the elongation at break of the various rubber compounds gradually increases with the mHNT content. The elongation at break of the nanocomposite was reduced as more mHNT was loaded into rubber composites. The elongation at break of the rubbery compound containing 10 phr of mHNT is slightly higher than the compounds containing 6 phr HNT and slightly higher than that of neat EPDM/NBR matrices, even though the increase in mHNT loading from 8 to 10 phr reduced the elongation at break of the resulting system. Composites' decreased elongation at break is the result of the rigid mHNT phase's presence in the rubber matrix, which increases the material's stiffness and strength.

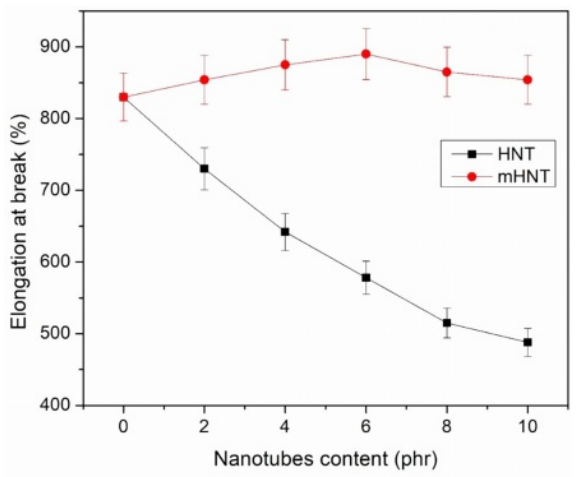

Figure 3. Elongation at break of EPDM/NBR blends with HNT and mHNT composites.

Tear Strength: Figure 4 demonstrates the tear strength of EPDM/NBR nanocomposites with different amounts of HNT. The inclusion of mHNT considerably increased the tear strength of EPDM/NBR composites. The tear pattern of NBR/montmorillonite (MMT) nanocomposites revealed a succession of tear ridges parallel to the tear direction, whereas unfilled NBR showed simple torn patterns, according to Kader *et al.*[72] They proposed that the tear path was varied along its length by uniformly scattered silicate layers and tiny tactoids, depending on the orientation of the silicate layers. As a result, there was more resistance to tear propagation. Due to interfacial contact and improved dispersion of mHNT compared to HNT, adding modified nanotubes resulted in better mechanical characteristics than adding HNT.

100% Modulus: The results of the 100 percent modulus of

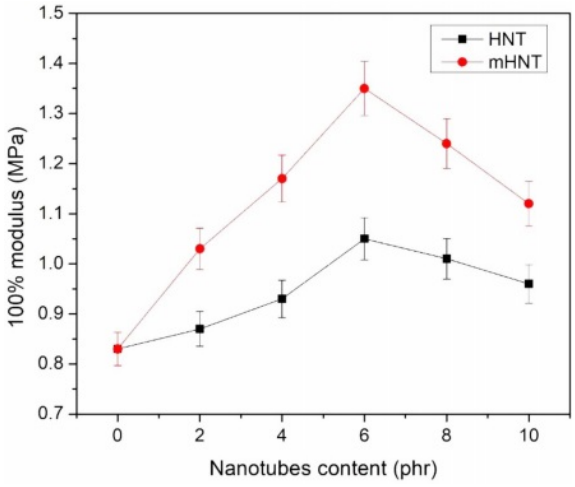

Figure 5. 100% modulus of EPDM/NBR blends with HNT and mHNT composites.

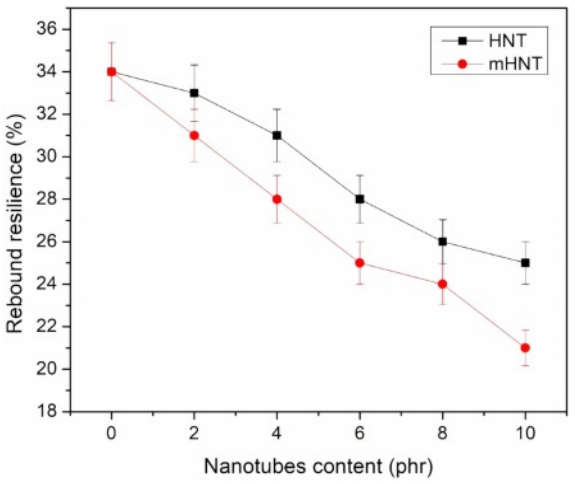

Figure 7. Rebound resilience of EPDM/NBR blends with HNT and mHNT composites.

the EPDM/NBR vulcanizate and its composites are shown in Figure 5. The 100 percent modulus of EPDM/NBR-HNT nanocomposites is significantly higher than that of basal EPDM/NBR blends. The mechanical properties of EPDM/NBR-mHNT nanocomposites are improved further by adding modified HNT at 100 percent modulus, tensile strength, and tear strength. The dispersion of nanotubes in EPDM/NBR matrix at the nanometer level, as well as the increase in crosslinking density caused by the reaction of EPDM/NBR and mHNT during the mixing and vulcanization processes, improve the interface properties and facilitate macromolecular intercalation into nanotubes, can be attributed to the reinforcing efficiency. The findings suggested that the high aspect ratio of nanotubes in nanocomposites and the reaction of RH on the surface of HNT in rubber matrix could not only reinforce rubber compounds, but also increase crosslinking density and improve interfacial adhesion between the EPDM/NBR and nanotubes, potentially improving the nanocomposites' mechanical properties.

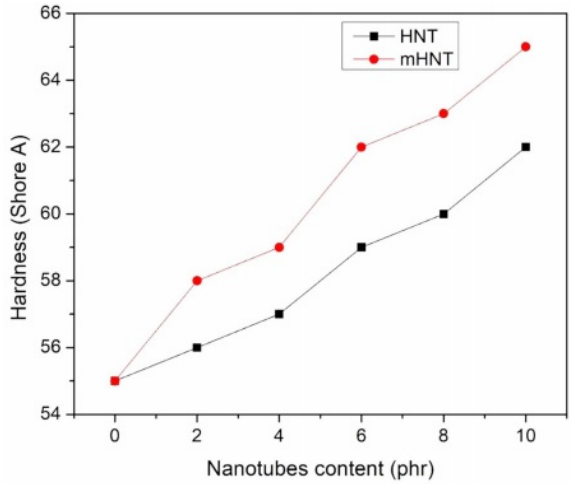

Figure 6. Hardness of EPDM/NBR blends with HNT and mHNT composites.

Hardness and Rebound Resilience: After adding mHNT to the nanocomposites, the hardness values of the nanocomposites changed. The Shore A hardness increased by 10 units with the addition of 10 phr mHNT (Figure 6). The modified HNT compounds have higher hardness values than the unmodified compounds with the same nanofiller loading. Figure 7 depicts the outcomes of rebound resilience studies. The rebound resilience did not change significantly, but the hardness increased dramatically with increasing levels of HNT, as shown in the Figure 7. Greater rebound resilience values are a common feature of EPDM/NBR rubber blends, and in this case, the HNT compounds have higher rebound resilience values due to their lower reinforcing efficiency. In terms of hardness, the rebound resilience of the mHNT filled nanocompounds is found to be better than the mHNT filled nanocompounds at the same HNT loading.

Abrasion Resistance: The abrasion property of the nanocomposites was assessed using a DIN type abrasion tester in accordance with ISO 4649. The average value from three specimens per sample was used to calculate the DIN volume loss for each sample. For tyres to function safely and have a long service life, abrasion resistance is essential. The abrasion resistance of rubbers, including thermoplastic elastomers and vulcanised thermoset rubbers, is measured by a DIN abrasion tester. A piece of rubber is moved against an abrasive material

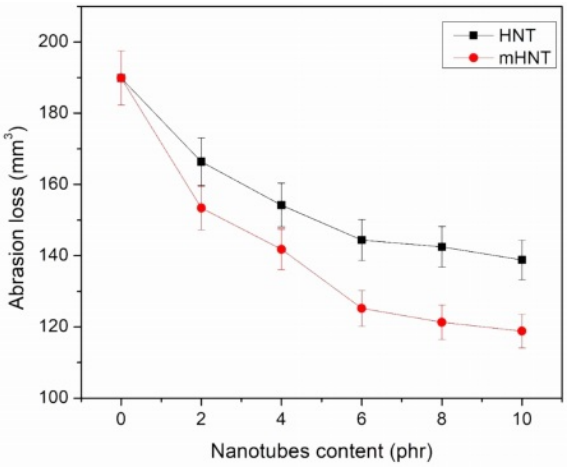

Figure 8. Abrasion loss of EPDM/NBR blends with HNT and mHNT composites.

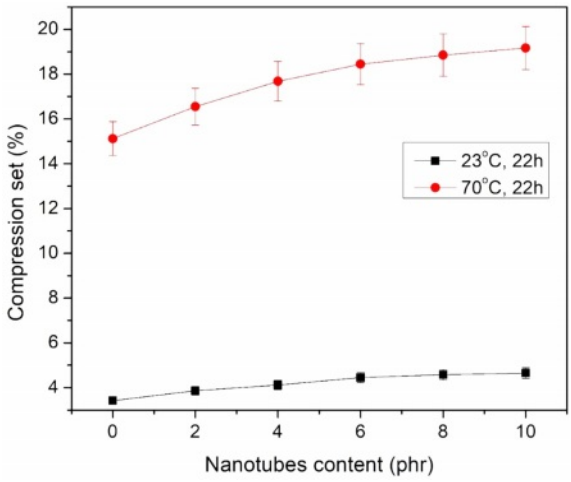

Figure 9. Compression set of EPDM/NBR-mHNT composites at different temperatures.

or sheet mounted on a rotating drum, commonly known as a rotary drum abrader, to conduct a DIN abrasion test. Volume loss in cubic millimetres is used to represent how much material will be removed during the abrasion process. A significant volume loss throughout the test indicates that the material is of poor quality and durability.

The DIN volume loss was used to determine the abrasion resistance of EPDM/NBR vulcanizates. Figure 8 illustrates the volume loss in DIN of EPDM/NBR-HNT and EPDM/NBR-mHNT vulcanizates with varying HNT concentrations. As the HNT level in EPDM/NBR-HNT vulcanizates increased, the volume loss of the vulcanizates decreased. Rubber abrasion is determined by its resistance to fracture or tearing when it comes into touch with sharp asperities. The addition of reinforcing fillers (such as CB) to traditional composites enhances abrasion resistance by preventing the polymer matrix from breaking.[73] EPDM/NBR-HNT vulcanizates contained tubular structure HNT morphologies, as previously stated. As a result, a larger concentration of HNT was more effective at preventing tearing of the EPDM/NBR rubber matrix. At a content of 10 phr, however, the addition of HNT only reduced EPDM/NBR DIN volume loss from 189.9 to 138.8 mm^3. In the case of EPDM/NBR-mHNT vulcanizates, the DIN volume loss of EPDM/NBR was significantly reduced for all mHNT concentrations. For unfilled EPDM/NBR rubber blends and EPDM/NBR having mHNT 2, 4, 6, 8, and 10 phr, DIN volume loss decreased from 189.9 to 153.4, 141.8, 125.2, 121.3, and 118.8 mm^3, respectively. This could be explained by the fact that mHNT has greater dispersion and distribution in the rubber matrix than EPDM/NBR-HNT, as evidenced by FESEM data and swelling behaviour, which will be described later. As a result of the greater RH agent bonding on mHNT particles compared to HNT particles, the interaction between mHNT nanofiller and EPDM/NBR rubber matrix was higher.

Compression Set. Figure 9 shows compression set data in relation to heat exposure period. Compression set, according to the definition, refers to how much the sample is permanently deformed. The RH treated HNT samples were chosen for the compression set because they had the best cure and mechanical properties. The effects of filler loading and temperature on the compression set of EPDM/NBR-mHNTs nanocomposite membranes are studied in this study. As the amount of mHNTs in EPDM/NBR nanocomposites increased, so did the compression set, which suggests that the sample seldom returns to its previous height as more mHNTs are incorporated into the EPDM/NBR matrix. This data also suggests that filled mHNTs composites interact with EPDM/NBR matrix more than unfilled mHNTs composites. Because the molecular motion of bound rubber generated near fillers is severely constrained, the proportion of EPDM/NBR matrix that contributes to elastic behaviour is reduced, and compression set increases as a result. Figure 9 demonstrates that for 10 phr mHNTs-filled EPDM/NBR composite samples at 70 °C, the compression set greatly increases after 22 h, and for 0, 2, 4, 6, 8 phr loading samples, the pattern was similar. The largest compression set was found in 10 phr mHNTs-filled EPDM/NBR nanocomposites under the measured temperature settings, and the memory retainable capacity was even lower than pure blend samples. At the early design stage, this approach can be utilised to estimate the safety and reliability design of vibration mount rubber mate-

rials.

Swelling Resistance. The ability of liquids to swell when passing across polymeric membranes is a significant regulating factor in many of their uses. In a range of applications such as reverse osmosis, pervaporation and food packaging, the swelling resistance of organic liquids through polymers is critical. The random molecular motion of individual molecules causes tiny molecules to swell through a polymer membrane. The free volume within the single rubber or rubber blends matrix, the nature of the compounds, crosslink density of the polymer materials, the nature of reinforcing fillers, geometry of the filler (size distribution, orientation, size, shape, and concentration), the penetrant size, temperature, interaction between the polymer matrix and reinforcing filler, and the amount of reinforcement all influence the diffusion process. Fillers play a big part in the swelling process.

The reason for selecting the RH treated HNT samples for the swelling resistance is due to its best cure and mechanical properties. The effects of penetrant size, filler loading, penetrant type, and temperature on the mole percent uptake of solvents *via* EPDM/NBR–mHNTs nanocomposite membranes are investigated in this study. The formula for calculating mole percent uptake is as follows:

$$Q_t \text{mol\%} = \left(\frac{\text{Mass of solvent sorbed/Molar mass of solvent}}{\text{Mass of polymer}}\right) \times 100 \quad (2)$$

Effect of Filler Loading: Figure 10 depicts xylene sorption curves through EPDM/NBR-mHNTs nanocomposites with various mHNT loadings. Because the concentration gradient of the penetrant in the nanocomposite is substantial, the swelling continues at a relatively rapid rate of solvent uptake. Due to the lower concentration gradient of the penetrant molecules, the rate of solvent uptake decreases. The figure also shows that the equilibrium uptake falls as the filler loading increases. 6 phr mHNT had the lowest solvent uptake, while untreated HNT loaded nanocomposite has the highest. This can be explained by the fact that after vulcanization, local mobility of the polymer is restricted by nanoscale mHNT reinforcement due to strong filler-polymer contact, causing the polymer chains to become less flexible, resulting in reduced sorption behaviour. The good dispersion of mHNTs in the rubber matrix is another cause for the decrease in solvent uptake for the 6 phr mHNT loaded sample. The homogeneous distribution of mHNTs in the rubber matrix restricts the transport of solvent through it as the amount of mHNTs increases. The solvent uptake rose marginally after 6 phr. This was related to the production of mHNT agglomerates, which can be seen in FESEM micrographs.

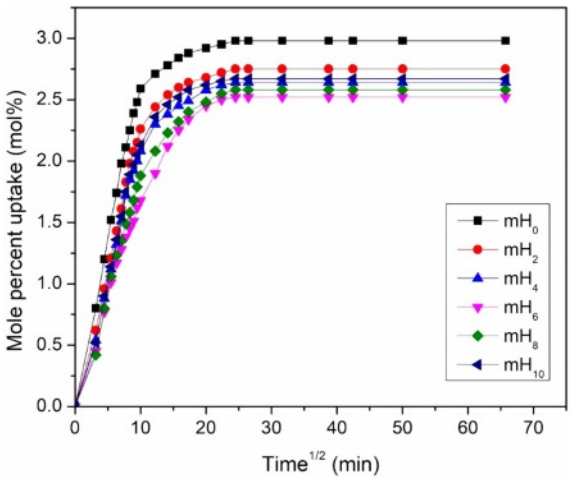

Figure 10. Mole percent uptake of xylene by different nanotubes loading at 30 °C.

The nanofiller's superior dispersion in the matrix enhances the surface area of the reinforcing phase, resulting in an excellent improvement in the nanocomposites' solvent resistance qualities. Figure 15 shows FESEM pictures that support this. In general, filler dispersion is critical in determining the performance of polymer-based composites. The amount of mHNTs required to develop an extensive network structure and show homogeneous distribution is relatively minimal at low concentrations of mHNTs. As a result, the solvent molecules are able to move through the matrix with ease. Figure 15(b) also shows that the mHNTs particles form a local filler-filler network in the rubber matrix. As a result, solvent molecules are unable to diffuse through the polymer. The free volume within the polymer matrix affects solvent molecule diffusion through the polymer membrane. With the addition of nanofillers, the free volume within the matrix reduces, resulting in a drop in equilibrium solvent uptake. Because the mHNTs take up the free volume of rubber, the density values increase as the filler loading increases, as shown in Table 3. The tortuosity of the route and the lower sorption area in the polymeric membrane in the presence of fillers can also explain the decrease in solvent uptake in filled systems.

Effect of the Nature of Solvent: The effect of penetrant size was investigated using a homologous series of aromatic, aliphatic, and chlorinated solvents. For the 6 phr mHNT filled sample, the swelling properties of EPDM/NBR-mHNTs nanocomposites in different solvents are examined and displayed in

Table 3. Mole Percent Uptake of Aromatic, Aliphatic and Chlorinated Penetrants of EPDM/NBR Blends Reinforced with HNT and mHNT Composites at 23 ºC, 40 ºC, 50 ºC and 60 ºC

Sample code (Sam)	Mole percent uptake (mol%) at 23 ºC										
	Aromatic				Aliphatic				Chlorinated		
	Benzene	Toluene	Xylene	Mesitylene	*n*-pentane	*n*-hexane	*n*-heptane	*n*-octane	Dichloro-methane	Chloroform	Carbon tetrachloride
mH_0	3.46	3.18	2.98	2.75	1.52	1.63	1.38	1.27	2.17	2.54	1.97
mH_2	3.28	3.07	2.75	2.54	1.35	1.48	1.32	1.17	2.09	2.42	1.94
mH_4	3.17	2.98	2.64	2.42	1.29	1.35	1.24	1.12	2.02	2.38	1.86
mH_6	3.03	2.89	2.52	2.28	1.23	1.28	1.17	1.06	1.95	2.32	1.77
mH_8	3.05	2.93	2.58	2.34	1.25	1.32	1.19	1.1	1.97	2.35	1.8
mH_{10}	3.14	2.96	2.67	2.39	1.27	1.36	1.22	1.14	2	2.39	1.83
Sam	Mole percent uptake (mol%) at 40 ºC										
mH_6	-	3.21	-	-	-	-	-	-	-	-	-
Sam	Mole percent uptake (mol%) at 50 ºC										
mH_6	-	3.54	-	-	-	-	-	-	-	-	-
Sam	Mole percent uptake (mol%) at 60 ºC										
mH_6	-	3.68	-	-	-	-	-	-	-	-	-

Figure 11. The mole percent uptake of solvents through composites shows a predictable tendency. Carbon tetrachloride has been reported to have a lower equilibrium absorption than dichloromethane and chloroform in chlorinated solvents. In aliphatic solvents, *n*-octane has been reported to have a lower equilibrium uptake than *n*-pentane, *n*-hexane, and *n*-heptane. Similarly, the equilibrium absorption of mesitylene in aromatic solvents has been reported to be lower than that of benzene, toluene, and xylene. Carbon tetrachloride's, *n*-octane's, and mesitylene's high molecular weight and molar volume may have contributed to their reduced equilibrium absorption in chlorinated, aliphatic, and aromatic solvents, respectively.

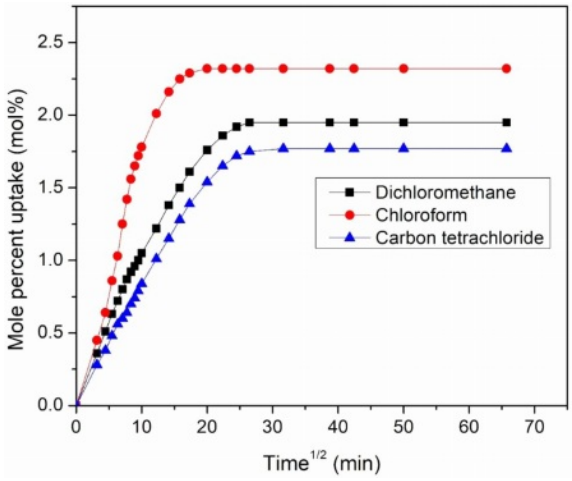

Figure 11. Mole percent uptake of different solvents through 6 phr mHNT filled EPDM/NBR nanocomposites.

In aliphatic solvents, the Q_t reduces as the molar volume and length of alkyl chains increase; in aromatic solvents, the Q_t drops as the phenyl group increases; and in chlorinated solvents, the Q_t decreases as the molar volume and length of the chlorine group increases. Aliphatic solvents have lower solvent absorption values than aromatic and chlorinated solvents due to their large molar volume.[74] Many researchers have documented a drop in Q_t as the size of the penetrant increases.[75,76] This is addressed by the free volume theory,[77] which states that a molecule's diffusion rate is highly influenced by the ease with which polymer chains interchange positions with solvent molecules. As the penetrant size grows larger, the ease of exchange decreases, especially in full matrices, resulting in a decrease in solvent absorption. Another explanation for inadequate solvent uptake is the high activation energy required for a big penetrant molecule.[78]

Effect of Temperature on Mole Percent Uptake: For the 6 phr mHNTs filler filled EPDM/NBR nanocomposite (mH_6), experiments are conducted at high temperatures (40, 50, and 60 ºC) in addition to room temperature to evaluate the effect of temperature on Qt characteristics. The mH_6 sample was chosen for the temperature research because it had the best solvent resistance at ambient temperature. Toluene was utilised as a solvent. Temperature has a substantial impact on Q_t values, as

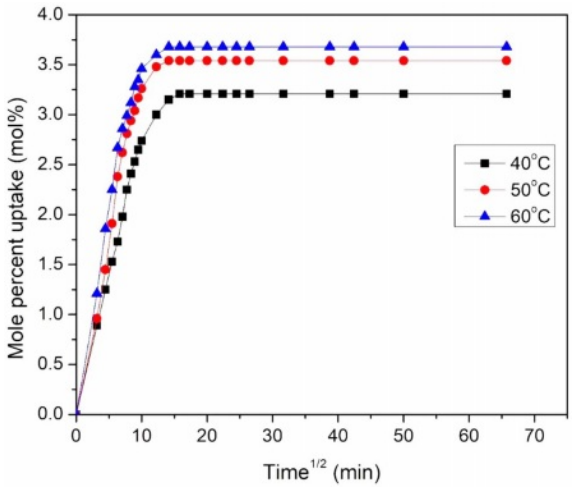

Figure 12. Temperature dependence of the 6 phr mHNT filled nanocomposites in toluene.

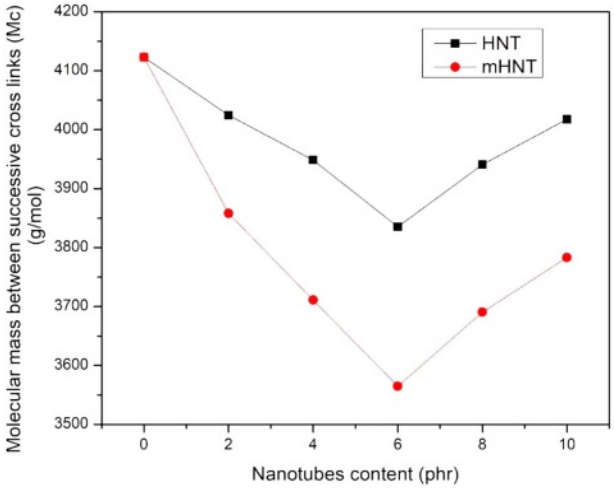

Figure 13. Molecular mass between successive cross links of EPDM/NBR blends with HNT and mHNT composites.

shown in Figure 12. At these temperatures, Q_t values suggest an increase in solvent uptake as the temperature rises. The slope of the linear part is likewise shown to rise with temperature, indicating that the swelling properties are temperature dependent. This can be attributed to an increase in free volume as a result of the polymer matrix's increased segmental motion, as well as the solvent molecules' gain in kinetic energy as a result of the higher number of collisions at high temperatures. Swelling is, thus, a temperature-dependent process.

Crosslink Density. The eq. (3) can be used to calculate the cross-link density.

$$v\left(\frac{\text{mol}}{\text{cm}^3}\right) = \frac{1}{2M_c} \tag{3}$$

where, v - crosslink density, M_c - Molecular mass between successive cross links. The Flory-Rehner equation can be used to calculate the molecular mass difference between successive crosslink.[79]

$$M_c = \frac{-\rho_p V_s V_r^{1/3}}{\ln(1-V_r)+V_r+\chi V_r^2} \tag{4}$$

where, V_s - molar volume of the solvent, ρ_p - density of the polymer, χ - interaction parameter of the polymer, and V_r - volume fraction of polymer in the solvent-swollen filled compound and is given by following eq.

$$V_r = \frac{1}{1+Q_m} \tag{5}$$

where, Q_m is the weight swell of the EPDM/NBR rubber nanocomposites in toluene solvent

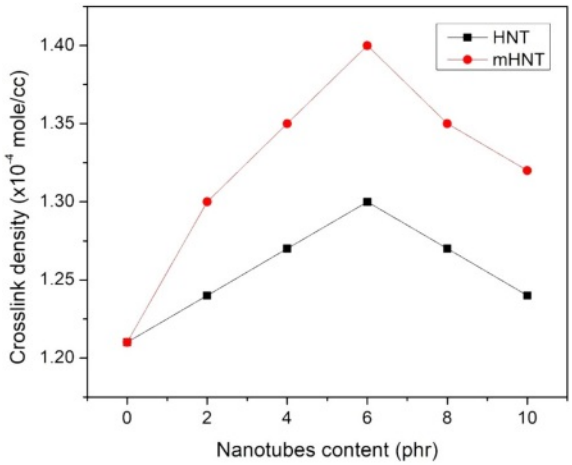

Figure 14. Crosslink density of EPDM/NBR blends with HNT and mHNT composites.

Values of M_c and v are given in Figure 13 and 14, respectively. The chart clearly shows that the M_c value for mH0 is the highest, indicating that mH_0 has the highest solvent absorption. As the M_c value drops from mH_0 to mH_8, the crosslink density of the samples varies. The value of M_c drops as the filler loading increases, indicating that the filler polymer interaction increases with filler loading and hence the maximum solvent absorption decreases. Because mH_0 has the highest M_c value, cross-links are far apart, allowing mH_0 to absorb the most solvent. In addition to the cross-links created by vulcanization, the nanofillers particles can contribute to the creation of cross-links. The accessible volume between consecutive cross-links diminishes as the M_c value falls.[80,81] The diffusion process is slowed as a result of this. Mc values for different nanofiller

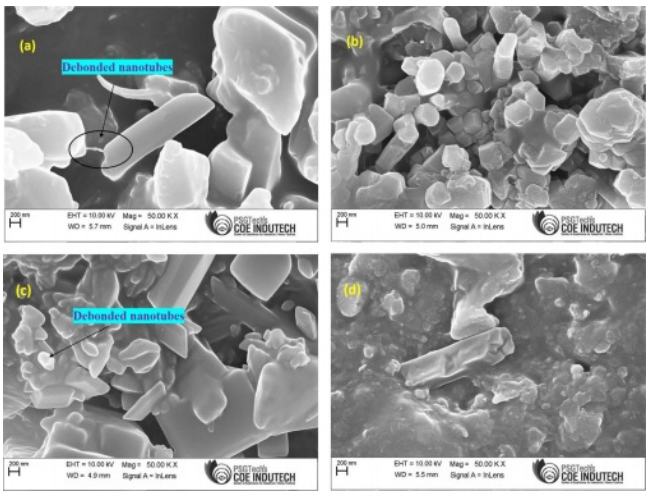

Figure 15. FESEM images showing the tensile fractured surfaces of nanotubes filled EPDM/NBR composites: (a) H_6; (b) mH_6; (c) H_{10}; (d) mH_{10}.

contents are as follows: $mH_0 > mH_2 > mH_4 > mH_6 < mH_8 < mH_{10}$ for a given solvent. The aggregation of the nanofiller, as seen in the FESEM micrographs, causes a modest rise in M_c at mHNTs content greater than 6 phr. The crosslink density increased as the nanofiller concentration in the composites increased,[82] with a peak value of 6 phr.

Effect of mHNT on the Morphology of EPDM/NBR-mHNT Nanocomposites. Figure 15 shows FESEM images of EPDM/NBR-HNT (75/25/6), EPDM/NBR/mHNT (75/25/6), EPDM/NBR-HNT (75/25/10) and EPDM/NBR-mHNT (75/25/10) nanocomposites. Figure 15(a) shows that EPDM/NBR-HNT nanocomposites contain a certain amount of HNT agglomerates. Furthermore, the interfaces between HNTs and the rubber matrix are visible, and several debonded nanotubes have been dragged out of the EPDM/NBR rubber matrix. This shows that HNTs and EPDM/NBR rubber matrix may have a weak interfacial interaction. In contrast to the EPDM/NBR-HNT nanocomposite shown in Figure 15(a), the EPDM/NBR-mHNT nanocomposites shown in Figure 15(b) have fewer agglomerates and most of the mHNTs particles are uniformly dispersed at the nanometer scale in the rubber matrix. The interfaces between mHNTs and the EPDM/NBR rubber matrix are also fuzzy, with hardly no debonded mHNTs. These findings imply that RH can boost the interfacial combination ability of mHNTs and EPDM/NBR rubber matrix, as well as facilitate their dispersion.

The FESEM micrographs of EPDM/NBR-HNT nanocomposites are shown in Figure 15(c). In EPDM/NBR-HNT nanocomposites, it was found that most HNTs were agglomerated, but the interfaces between the HNTs and the EPDM/NBR were clear and numerous debonded HNTs were discovered, which is explained by the ineffective interfacial contact between the filler and the polymer. However, upon modification, the HNTs were uniformly distributed throughout the EPDM/NBR matrix (Figure 15(d)), and there were fewer agglomerates than in the unmodified HNT-filled nanocomposites. Because the filler and matrix had high interfacial contact, the interfaces between HNTs and EPDM/NBR were therefore undetectable. The improved dispersion and more HNTs implanted in the EPDM/NBR matrix were responsible for the modified nanocomposites' greater tensile characteristics. These findings imply that RH not only expands the distribution of HNTs within the matrix but also expands the contact between the filler and the polymer at the interface, as shown by the crosslinking density data.

Conclusions

The sulphur vulcanization reaction of EPDM/NBR rubber vulcanizates was accelerated by both mHNT and HNT. When mHNT or HNT were added to EPDM/NBR, the mechanical characteristics, abrasion resistance, and swelling resistance of the resultant rubber nanocomposites improved. The abrasion and swelling resistance of EPDM/NBR nanocomposites improved more than that of HNT-EPDM/NBR nanocomposites due to surface modification and greater mHNT dispersion. Mechanical characteristics of EPDM/NBR-mHNT nanocomposites improved as mHNT content increased, but mechanical properties of EPDM/NBR-HNT nanocomposites remained unaltered when HNT content increased.

Acknowledgements: The authors are highly grateful to E.G.S. Pillay Engineering College, Nagappattinam & SA Engineering college, Chennai, India for their kind support in providing the time for research for academic interest.

Conflict of Interest: The authors declare that there is no conflict of interest.

References

1. Medalia, A. Effect of Carbon Black on Dynamic Properties of Rubber Vulcanizates. *Rubber Chem. Technol.* **1978**, 51, 437-523.
2. Vilgis, T. A.; Heinrich, G. Disorder-induced Enhancement of Polymer Adsorption-A Model for the Rubber-polymer Interaction

in Filled Rubbers. *Macromolecules* **1994**, 27, 26.
3. Senthilvel, K.; Vishvanathperumal, S.; Prabu, B.; Baruch, L. J. Studies on the Morphology, Cure Characteristics anD Mechanical Properties of Acrylonitrile Butadiene Rubber with Hybrid Iller (carbon black/silica) Composite. *Polym. Polym. Compos.* **2016**, 24, 473-480.
4. Vishvanathperumal, S.; Gopalakannan, S. Reinforcement of Ethylene Vinyl Acetate with Carbon Black/silica Hybrid Filler Composites. *Appl. Mech. Mater.* **2016**, 852, 16-22.
5. Merabia, S.; Sotta, P.; Long, D. R. A Microscopic Model for the Reinforcement and the Nonlinear Behavior of Filled Elastomers and Thermoplastic Elastomers (Payne and Mullins Effects). *Macromolecules* **2008**, 41, 8252-8266.
6. Anand, G.; Vishvanathperumal, S. Properties of SBR/NR Blend: The Effects of Carbon Black/Silica (CB/SiO_2) Hybrid Filler and Silane Coupling Agent. *Silicon* **2022**, 14, 9051-9060.
7. Vishvanathperumal, S.; Navaneethakrishnan, V.; Anand, G.; Gopalakannan, S. Evaluation of Crosslink Density Using Material Constants of Ethylene-Propylene-Diene Monomer/Styrene-Butadiene Rubber with Different Nanoclay Loading: Finite Element Analysis-simulation and Experimental. *Adv. Sci. Eng. Med.* **2020**, 12, 632-642.
8. Vishvanathperumal, S.; Anand, G. Effect of Nanosilica and Crosslinking System on the Mechanical Properties and Swelling Resistance of EPDM/SBR Nanocomposites with and without TESPT. *Silicon* **2021**, 13, 3473-3497.
9. Sadasivuni, K. K.; Ponnamma, D.; Thomas, S.; Grohens, Y. Evolution from Graphite to Graphene Elastomer Composites. *Prog. Polym. Sci.* **2014**, 39, 749-780.
10. Paran, S. M. R.; Naderi, G.; Ghoreishy, M. H. R. XNBR-grafted Halloysite Nanotubes Core-Shell as a Potential Compatibilizer for Immiscible Polymer Systems. *Appl. Surf. Sci.* **2016**, 382, 63-72.
11. Tripathi, B. P.; Shahi, V. K. ChemInform Abstract: Organic-Inorganic Nanocomposite Polymer Electrolyte Membranes for Fuel Cell Applications. *Prog. Polym. Sci*. **2011**, 36, 945-979.
12. Haraguchi, K.; Li, H. J. Mechanical Properties and Structure of Polymer-Clay Nanocomposite Gels with High Clay Content. *Macromolecules* **2006**, 39, 1898-1905.
13. Anirudhan, T.S.; Alexander, S. Multiwalled Carbon Nanotube Based Molecular Imprinted Polymer for Trace Determination of 2,4-Dichlorophenoxyaceticacid in Natural Water Samples Using a Potentiometric Method. *Appl. Surf. Sci*. **2014**, 303, 180-186.
14. Ganeche, P. S.; Balasubramanian, P.; Vishvanathperumal, S. Halloysite Nanotubes (HNTs)-Filled Ethylene-Propylene-Diene Monomer/Styrene-Butadiene Rubber (EPDM/SBR) Composites: Mechanical, Swelling, and Morphological Properties. *Silicon*, **2021**, 14, 6611-6620.
15. Yah, W. O.; Takahara, A.; Lvov, Y. M. Selective Modification of Halloysite Lumen with Octadecylphosphonic Acid: New Inorganic Tubular Micelle. *J. Am. Chem. Soc.* **2012**, 134, 1853-1859.
16. Abdullayev, E.; Joshi, A.; Wei, W.; Zhao, Y.; Lvov, Y. Enlargement of Halloysite Clay Nanotube Lumen by Selective Etching of Aluminum Oxide. *ACS Nano* **2012**, 6, 7216-7226.
17. Liu, M.; Jia, Z.; Jia, D.; Zhou, C. Recent Advance in Research on Halloysite Nanotubes-Polymer Nanocomposite. *Prog. Polym. Sci.* **2014**, 39, 1498-1525.
18. Liu, M.; Guo, B.; Du, M.; Cai, X.; Jia, D. Properties of Halloysite Nanotube Epoxy Resin Hybrids and the Interfacial Reactions in the Systems. *Nanotechnology* **2007**, 18, 89-99.
19. Cavallaro, G.; Lazzara, G.; Milioto, S.; Palmisano, G.; Parisi, F. Halloysite Nanotubes with Fluorinated Lumen: Non-foaming Nanocontainer for Storage and Controlled Release of Oxygen in Aqueous Media. *J. Colloid Interface Sci.* **2014**, 417, 66-71.
20. Liu, M.; Jia, Z.; Jia, D.; Zhou, C. Recent Advance in Research on Halloysite Nanotubes Polymer Nanocomposite. *Prog. Polym. Sci.* **2014**, 39, 1498-1525.
21. Solomon, D. H. Clay Minerals as Electron Acceptors and/or Electron Donors in Organic Reactions. *Clay Clay Miner.* **1968**, 16, 31-39.
22. Rawtani, D.; Agrawal, Y. K. Multifarious Applications of Halloysite Nanotubes: A Review. *Rev. Adv. Mater. Sci.* **2012**, 30, 282-295.
23. Cavallaro, G.; Lazzara, G.; Milioto, S. Sustainable Nanocomposites Based on Halloysite Nanotubes and Pectin/polyethylene Glycol Blend. *Polym. Degrad. Stab.* **2013**, 98, 2529-2536.
24. Cavallaro, G.; Lisi, R. D.; Lazzara, G.; Milioto, S. Polyethylene Glycol/Clay Nanotubes Composites Thermal Properties and structure. *J. Therm. Anal. Calorim.* **2013a**, 112, 383-389.
25. Deen, I.; Zhitomirsky, I. Electrophoretic Deposition of Composite Halloysite Nanotubes-Hydroxyapatite-Hyaluronic Acid Films. *J. Alloys Compd.* **2014**, 586, S531-S534.
26. Du, Y.; Zheng, P. Adsorption and Photodegradation of Methylene Blue on TiO_2-halloysite Adsorbents. *Korean J. Chem. Eng.* **2014**, 31, 2051-2056.
27. Yuan, P.; Tan, D.; Bergaya, F. A. Properties and Applications of Halloysite Nanotubes: Recent Research Advances and Future Prospects. *Appl. Clay Sci.* **2015**, 112-113, 75-93.
28. Yuan, P.; Southon, P. D.; Liu, Z.; Green, M. E. R.; Hook, J. M.; Antill, S. J.; Kepert, C. J. Functionalization of Halloysite Clay Nanotubes by Grafting with γ-aminopropyltriethoxysilane. *J. Phys. Chem. C* **2008**, 112, 15742-15751.
29. Hashemifard, S. A.; Ismail, A. F.; Matsuura, T. Mixed Matrix Membrane Incorporated with Large Pore Size Halloysite Nanotubes (HNT) as Filler for Gas Separation: Experimental. *J. Colloid Interface Sci.* **2011**, 359, 359-370.
30. Zhao, Y.; Abdullayev, E.; Vasiliev, A.; Lvov, Y. Halloysite Nanotubule Clay for Efficient Water Purification. *J. Colloid Interface Sci.* **2013**, 406, 121-129.
31. Abdullayev, E.; Sakakibara, K.; Okamoto, K.; Wei, W.; Ariga, K.; Lvov, Y. Natural Tubule Clay Template Synthesis of Silver Nanorods for Antibacterial Composite Coating. *ACS Appl. Mater. Interfaces* **2011**, 3, 4040-4046.
32. Jia, Z.; Luo, Y.; Guo, B.; Yang, B.; Du, M.; Jia, D. Reinforcing and Flame Retardant Effects of Halloysite Nanotubes on LLDPE. *Polym.-Plast. Technol. Eng.* **2009**, 48, 607-613.
33. Pasbakhsh, P.; Churchman, G. J.; Keeling, J. L. Characterisation

of Properties of Various Halloysites Relevant to Their Use as Nanotubes and Microfibre Fillers. *Appl. Clay Sci.* **2013**, 74, 47-57.
34. Rooj, S.; Das, A.; Thakur, V.; Mahaling, R. N.; Bhowmick, A. K.; Heinrich, G. Preparation and Properties of Natural Nanocomposites Based on Natural Rubber and Naturally Occurring Halloysite Nanotubes. *Mater. Des.* **2010**, 31, 2151-2156.
35. Du, M.; Guo, B.; Lei, Y.; Liu, M.; Jia, D. Carboxylated Butadiene-Styrene Rubber/halloysite Nanotube Nanocomposites: Interfacial Interaction and Performance. *Polymer* **2008**, 49, 4871-4876.
36. Cavallaro, G.; Lazzara, G.; Milioto, S. Dispersions of Nanoclays of Different Shapes into Aqueous and Solid Biopolymeric Matrices. Extended Physicochemical Study. *Langmuir* **2010**, 27, 1158-1167.
37. Arcudi, F.; Cavallaro, G.; Lazzara, G. Selective Functionalization of Halloysite Cavity by Click Reaction: Structured Filler for Enhancing Mechanical Properties of Bionanocomposite Films. *J. Phys. Chem. C* **2014**, 118, 15095-15101.
38. Liu, M.; Guo, B.; Zou, Q.; Du, M.; Jia, D. Interactions Between Halloysite Nanotubes and 2,5-Bis(2-benzoxazolyl) Thiophene and Their Effects on Reinforcement of Polypropylene/Halloysite Nanocomposites. *Nanotechnology* **2008**, 19, 205709-205709.
39. Liu, M.; Chang, Y.; Yang, J.; You, Y.; He, R.; Chen, T.; Zhou, C. Functionalized Halloysite Nanotube by Chitosan Grafting for Drug Delivery of Curcumin to Achieve Enhanced Anticancer Efficacy. *J. Mater. Chem. B* **2016**, 4, 2253-2263.
40. Liu, M.; Wu, C.; Jiao, Y.; Xiong, S.; Zhou, C. Chitosanehalloysite Nanotubes Nanocomposite Scaffolds for Tissue Engineering. *J. Mater. Chem. B* **2013**, 1, 2078-2089.
41. Ye, Y.; Chen, H.; Wu, J.; Ye, L. High Impact Strength Epoxy Nanocomposites with Natural Nanotubes. *Polymer* **2007**, 48, 6426-6433.
42. Liu, M.; Guo, B.; Du, M.; Cai, X.; Jia, D. Properties of Halloysite Nanotubes-Epoxy Resin Hybrids and the Interfacial Reactions in the Systems. *Nanotechnology* **2007**, 18, 281-287.
43. Marney, D. C. O.; Russell, L. J.; Wu, D. Y.; Nguyen, T.; Cramm, D.; Rigopoulos, N.; Wright, N.; Greaves, M. The Suitability of Halloysite Nanotubes as a Fire Retardant for Nylon 6. *Polym. Degrad. Stab.* **2008**, 93, 1971-1978.
44. Zhao, M.; Liu, P. Preparation of Halloysite Nanotubes/Polystyrene (HNTs/PS) Core-Shell Particles *via* Soap-Less Microemulsion Polymerization. *J. Macromol. Sci. Part B Phys.* **2007**, 46, 891-897.
45. Jia, Z.; Luo, Y.; Guo, B.; Yang, B.; Du, M.; Jia, D. Reinforcing and Flame-Retardant Effects of Halloysite Nanotubes on LLDPE. *Polymer-Plastics Technol. Eng.* **2009**, 48, 607-613.
46. Liu, M.; Guo, B.; Du, M.; Jia, D. Drying Induced Aggregation of Halloysite Nanotubes in Polyvinyl Alcohol/Halloysite Nanotubes Solution and Its Effect on Properties of Composite Film. *Appl. Phys. A* **2007**, 88, 391-395.
47. Liu, C.; Luo, Y. F.; Jia, Z. X.; Zhong, B. C.; Li, S. Q.; Guo, B. C.; Jia, D. M. Enhancement of Mechanical Properties of Poly(vinyl chloride) with Polymethyl Methacrylate-Grafted Halloysite Nanotube. *Express Polym. Lett.* **2011**, 5, 591-603.
48. Jia, Z.; Guo, B.; Jia, D. Advances in Rubber/Halloysite Nanotubes Nanocomposites. *J. Nanosci. Nanotechnol.* **2014**, 14, 1758-1771.
49. Liu, M.; Jia, Z.; Jia, D.; Zhou, C. Recent Advance in Research on Halloysite Nanotubes-Polymer Nanocomposite. *Prog. Polym. Sci.* **2014**, 39, 1498-1525.
50. Hayeemasae, N.; Sensem, Z.; Surya, I.; Sahakaro, K.; Ismail, H. Synergistic Effect of Maleated Natural Rubber and Modified Palm Stearin as Dual Compatibilizers in Composites Based on Natural Rubber and Halloysite Nanotubes. *Polymers* **2020**, 12, 766.
51. Ismail, H.; Salleh, S. Z.; Ahmad, Z. Curing Characteristics, Mechanical, Thermal, and Morphological Properties of Halloysite Nanotubes (HNTs)-filled Natural Rubber Nanocomposites. *Polymer-Plastics Technol. Eng.* **2011**, 50, 681-688.
52. Lei, Y.; Tang, Z.; Zhu, L.; Guo, B.; Jia, D. Functional Thiol Ionic Liquids as Novel Interfacial Modifiers in SBR/HNTs Composites. *Polymer* **2011**, 52, 1337-1344.
53. Du, M.; Guo, B.; Lei, Y.; Liu, M.; Jia, D. Carboxylated Butadieneestyrene Rubber/Halloysite Nanotube Nanocomposites: Interfacial Interaction and Performance. *Polymer* **2008**, 49, 4871-4876.
54. Rybinski, P.; Janowska, G.; Jozwiak, M.; Paja¸ A. K. Thermal Properties and Flammability of Nanocomposites Based on Diene Rubbers and Naturally Occurring and Activated Halloysite Nanotubes. *J. Therm. Analysis Calorim.* **2012**, 107, 1243-1249.
55. Ismail, H.; Pasbakhsh, P.; Fauzi, M. N. A.; Bakar, A. A. Morphological, Thermal and Tensile Properties of Halloysite Nanotubes Filled Ethylene Propylene Diene Monomer (EPDM) Nanocomposites. *Polym. Test. Polym. Test.* **2008**, 27, 841-850.
56. Pasbakhsh, P.; Ismail, H.; Fauzi, M. N. A.; Bakar, A. A. Influence of Maleic Anhydride Grafted Ethylene Propylene Diene Monomer (MAH-*g*-EPDM) on the Properties of EPDM Nanocomposites Reinforced by Halloysite Nanotubes. *Polym. Test.* **2009**, 28, 548-559.
57. Pasbakhsh, P.; Ismail, H.; Fauzi, M. N. A.; Bakar, A. A. EPDM/Modified Halloysite Nanocomposites. *Appl. Clay Sci.* **2010**, 48, 405-413.
58. Rooj, S.; Das, A.; Heinrich, G. Tube-like Natural Halloysite/Fluoroelastomer Nanocomposites with sImultaneous Enhanced Mechanical, Dynamic Mechanical and Thermal Properties. *Eur. Polym. J.* **2011**, 47, 1746-1755.
59. Jia, Z.-X.; Luo, Y.-F.; Yang, S.-Y.; Guo, B.-C.; Du, M.-L.; Jia, D.-M. Morphology, Interfacial Interaction and Properties of Styrene-butadiene Rubber/Modified Halloysite Nanotube Nanocomposites. *Chin. J. Polym. Sci.* **2011**, 27, 857-864.
60. Jia, Z.; Luo, Y.; Yang, S.; Du, M.; Guo, B.; Jia, D. Styrene-Butadiene Rubber/Halloysite Nanotubes Composites Modified by Epoxidized Natural Rubber. *J. Nanosci. Nanotechnol.* **2011**, 11, 10958-10962.
61. Guo, B.; Lei, Y.; Chen, F.; Liu, X.; Du, M.; Jia, D. Styreneebutadiene Rubber/Halloysite Nanotubes Nanocomposites Modified by Methacrylic Acid. *Appl. Surf. Sci.* **2008**, 255, 2715-2722.
62. Guo, B.; Chen, F.; Lei, Y.; Liu, X.; Wan, J.; Jia, D. Styrene-Butadiene Rubber/Halloysite Nanotubes Nanocomposites

Modified by Sorbic Acid. *Appl. Surf. Sci*. **2009**, 255, 7329-7336.
63. Hwang, W. G.; Wei, K. H. Mechanical Thermal and Barrier Properties of NBR /Organosilicate Nanocomposites. *Polym. Eng. Sci*. **2004**, 44, 2117-2124.
64. Mao, X.; Xu, S.; Wu, C. Dynamic Mechanical Properties of EPDM Rubber Blends. *Polym.-Plast. Technol. Eng.* **2008**, 47, 209-214.
65. Botros, S. H.; Tawfic, M. L. Compatibility and Thermal Stability of EPDM-NBR Elastomer Blends. *J. Elasto. Plast.* **2005**, 37, 299-317.
66. AL-Gahtani, S. A. Mechanical Properties of Acrylonitrile Butadiene/Ethylene Propylene Diene Monomer Blends: Effects of Blend Ratio and Filler Addition. *J. Am. Sci.* **2011**, 7, 804-809.
67. Theja, R.; Kilari, N.; Vishvanathperumal, S.; Navaneethakrishnan, V. Modeling Tensile Modulus of Nanoclay-Filled Ethylene-Propylene-Diene Monomer/Styrene-Butadiene Rubber Using Composite Theories. *J. Rubber Res.* **2021**, 24, 847-856.
68. Vishvanathperumal, S.; Navaneethakrishnan, V.; Gopalakannan, S. The Effect of Nanoclay and Hybrid Iller on Curing Characteristics, Mechanical Properties and Swelling Resistance of Ethylene Vinyl Acetate/Styrene Butadiene Rubber Blend Composite. *J. Adv. Microsc. Res.* **2018**, 13, 469-476.
69. Vishvanathperumal, S.; Gopalakannan, S. Swelling Properties, Compression Set Behavior and Abrasion Resistance of Ethylene-propylene-diene Rubber/Styrene Butadiene Rubber Blend Nanocomposites. *Polym. Korea* **2017**, 41, 433-442.
70. Jia, Z.-X.; Luo, Y.-F.; Yang, S.-Y.; Guo, B.-C.; Du, M.-L.; Jia, D.-M. Morphology, Interfacial Interaction and Properties of Styrene-butadiene Rubber/Modified Halloysite Nanotubes Nanocomposites. *Chinese J. Polym. Sci.* **2009**, 27, 857-864.
71. Liu, L.; Jia, D. M.; Luo, Y. F.; Guo, B. C. Preparation, Structure and Properties of Nitrile-butadiene Rubber-organoclay Nanocomposites by Reactive Mixing Intercalation Method. *J. Appl. Polym. Sci.* **2006**, 100, 1905-1913.
72. Kader, M.; Kim, K.; Lee, Y.-S.; Nah, C. Preparation and Properties of Nitrile Rubber/Montmorillonite Nanocomposites *via* Latex Blending. *J. Mater. Sci.* **2006**, 41, 7341-7352.
73. Gent, A. N.; Pulford, C. T. R. Mechanisms of Rubber Abrasion. *J. Appl. Polym. Sci.* **1983**, 28, 943-960.
74. Seehra, M. S.; Yalamanchi, M.; Singh, V. Structural Characteristics and Swelling Mechanism of Two Commercial Nitrile-butadiene Elastomers in Various Fluids. *Polym. Test.* **2012**, 4, 564-571.
75. Lucht, L. M.; Peppas, N. A. Transport of Penetrants in the Macromolecular Structure of Coals. V. Anomalous Transport in Pretreated Coal Particles. *J. Appl. Polym. Sci*. **1987**, 33, 1557-1566.
76. Aminabhavi, T. M.; Khinnavar, R. S. Diffusion and Sorption of Organic Liquids Through Polymer Membranes: 10. Polyurethane, Nitrile-butadiene Rubber and Epichlorohydrin Versus Aliphatic Alcohols (C1-C5). *Polymer* **1993**, 34, 1006-1018.
77. Stephen, R.; Joseph, K.; Oommen, Z.; Thomas, S. Molecular Transport of Aromatic Solvents Through Microcomposites of Natural Rubber (NR), Carboxylated Styrene Butadiene Rubber (XSBR) and Their Blends. *Compos. Sci. Technol.* **2007**, 67, 1187-1194.
78. Unnikrishnan, G.; Thomas, S. Molecular Transport of Benzene and Methyl-substituted Benzenes into Filled Natural Rubber Sheets. *J. Appl. Polym. Sci*. **1996**, 60, 963-970.
79. Flory, P. J.; Rehner, J. Statistical Mechanics of Cross-Linked Polymer Networks I. Rubberlike Elasticity. *J. Chem. Phys.* **1943**, 11, 512-521.
80. Vishvanathperumal, S.; Gopalakannan, S. Effects of the Nanoclay and Crosslinking Systems on the Mechanical Properties of Ethylene-Propylene-Diene Monomer/styrene Butadiene Rubber Blends Nanocomposite. *Silicon* **2019**, 11, 117-135.
81. Vishvanathperumal, S.; Anand, G. Effect of Nanoclay/Nanosilica on the Mechanical Properties, Abrasion and Swelling Resistance of EPDM/SBR Composites. *Silicon* **2020**, 12, 1925-1941.
82. Vishvanathperumal, S.; Anand, G. Effect of Nanosilica on the Mechanical Properties, Compression Set, Morphology, Abrasion and Swelling Resistance of Sulphur Cured EPDM/SBR Composites. *Silicon* **2022**, 14, 3523-3534.